DISCRETE AND CONTINUOUS
DYNAMICAL SYSTEMS
Supplement Volume 2005

Website: http://AIMsciences.org

pp. **131–141**

RENORMALIZATION GROUP CALCULATION OF ASYMPTOTICALLY SELF-SIMILAR DYNAMICS

Gastão A. Braga

Departamento de Matemática
Universidade Federal de Minas Gerais, Brazil

Frederico Furtado

Department of Mathematics
University of Wyoming, USA

Vincenzo Isaia

Department of Mathematics
Alfred State College, NY, USA

Abstract. We present a systematic numerical procedure for the computation of asymptotically self-similar dynamics of physical systems whose evolution is modeled by PDEs. This approach is based on the renormalization group (RG) for PDEs, which was originally introduced by N. Goldenfeld, Y. Oono and collaborators, and was further developed by J. Bricmont, A. Kupiainen and collaborators. We explain how successive iterations of a discrete RG transformation in space and time drive the system towards a fixed point, which corresponds to a self-similar dynamics. The iteration of the RG transformation renders explicit the relative importance of the distinct physical effects being modeled in the long-time dynamics. The resulting numerical procedure is very efficient and provides a detailed picture of the asymptotics, including scaling exponents, profile functions, and prefactors. We illustrate the effectiveness of the procedure on a set of examples of nonlinear PDEs, including cases where nonlinear effects are asymptotically irrelevant or neutral. In the latter case the asymptotic scaling laws obeyed by the dynamics frequently contain logarithmic corrections, which are detected and successfully handled by the RG procedure.

1. **Introduction.** There are many PDEs of interest in science whose solutions evolve to a self-similar form in certain asymptotic limits (large-time behavior, finite blow-up or extinction times). Numerous examples can be found in the book [2]. When this happens, the solutions simplify and their behavior can be characterized in terms of a small number of significant parameters. For instance, if the large-time asymptotic limit of a solution u is self-similar,

$$u(x,t) \sim \frac{A}{t^{\alpha}}\,\phi\left(B\frac{x}{t^{\beta}}\right), \quad \text{as } t \to \infty.$$

In this case, the large-time behavior is essentially described by the two scaling exponents α and β: α represents the rate of decay of the magnitude of u, while β is

2000 *Mathematics Subject Classification.* Primary: 35K55, 35B40, 35B33, 35B27; Secondary: 74S20.

Key words and phrases. Renormalization group, self-similar dynamics, asymptotic behavior, partial differential equations.

This work is partially supported by NSF.

the rate of spread of the space distribution of u, given by the profile ϕ, with time. The constants A and B provide additional information about the behavior, since they are usually related to underlying conservation laws satisfied by solutions.

It turns out that often such a self-similar behavior possesses a great deal of universality: the scaling exponents α and β and the profile ϕ are independent of initial conditions or even of the form of the equations (within respective suitable classes). The effects of such details are manifest only in the constants A and B.

Universal behavior is a central issue in the study of critical phenomena in equilibrium statistical mechanics and quantum field theory. Using the renormalization group (RG) approach [17, 29, 24, 18], physicists predict critical exponents and determine the universality class of a variety of models. In the early 1990s, Goldenfeld, Oono and collaborators developed a perturbative renormalization group method for PDEs and applied it to the study of a number of difficult long-time asymptotic problems [19, 14, 20]. A detailed account of this method can be found in [18]. See also [11, 12, 25] for a slight twist of the original method. Subsequently, Bricmont, Kupiainen and Lin [8, 9] introduced a nonperturbative renormalization group approach. A numerical renormalization group algorithm was developed at the same time by Chen and Goldenfeld [13] and was later adapted by Aronson and collaborators to study focusing solutions of the porous medium equation [4, 1]. See [15] and references therein for an interesting discussion of the relation between renormalization groups, problem reduction and optimal prediction algorithms.

In the present paper we combine the numerical approach of Chen and Goldenfeld with the RG approach of Bricmont et al. to develop a systematic numerical procedure for the calculation of asymptotically self-similar dynamics. The resulting numerical procedure is very efficient and provides a detailed picture of the asymptotics, including scaling exponents, profile functions, and scaling factors. In addition, this procedure renders explicit the relative importance of the distinct effects represented by the terms in the equations in the long-time dynamics.

Numerical procedures based on rescaling, and thus similar in spirit to the RG approach presented here, have previously been developed [22, 3] and used to study solutions which blow up in finite time. Such procedures exploit the known self-similar structure of the solutions under study to define the appropriate rescalings. Recently, versatile and more efficient versions of such procedures were developed [26, 16] and employed for the computation of solutions which blow up at multiple points. Yet the RG procedure presented here is unique in exploiting fixed points. On the other hand the current implementation of this procedure is not appropriate for studying blow-up problems.

2. **Scaling transformations.**

The RG method for PDEs is simply the integration of the equations over a finite time-interval with fixed length followed by a rescaling. To explain this idea, we need some preliminary notions. After these, the numerical RG procedure will be taken up in detail.

Let u be a global solution of the initial value problem (IVP)

$$\begin{cases} \partial_t u = N(x,t,u,\partial_x u,\partial_x^2 u,\dots), \quad x\in\mathbb{R},\, t>1, \\ u(x,1)=f(x), \quad x\in\mathbb{R}. \end{cases} \tag{1}$$

For a fixed $L>1$ and sequences $\{\alpha_n\}$ and $\{\beta_n\}$ of scaling exponents, define the sequence $\{u_n\}$ of rescaled functions inductively by

$$u_0=u, \quad u_n(x,t)=L^{\alpha_n}u_{n-1}(L^{\beta_n}x,Lt) \quad (n\geq 1). \tag{2}$$

Then u_n satisfies the *renormalized* IVP

$$\begin{cases} \partial_t u_n = N_n(x,t,u_n,\partial_x u_n,\partial_x^2 u_n,\dots), \quad x\in\mathbb{R},\ t>1, \\ u_n(x,1) = f_n(x), \quad x\in\mathbb{R}, \end{cases} \tag{3}$$

where $f_n(x) = L^{\alpha_n} u_{n-1}(L^{\beta_n}x, L)$, $N_0 = N$, and for $n \geq 1$ $N_n(x,t,u,p,q,\dots) = L^{1+\alpha_n} N_{n-1}\left(L^{\beta_n}x, Lt, L^{-\alpha_n}u, L^{-(\alpha_n+\beta_n)}p, L^{-(\alpha_n+2\beta_n)}q,\dots\right)$. Moreover, the inductive construction of u_n, see (2), yields the following relation:

$$u_n(x,t) = L^{n\overline{\alpha}_n} u\left(L^{n\overline{\beta}_n}x, L^n t\right), \tag{4}$$

where $\overline{\alpha}_n = (\alpha_1 + \cdots + \alpha_n)/n$ and $\overline{\beta}_n$ is defined similarly. In particular, u_n in the time interval $t \in [1, L]$ relates to u in $t \in [L^n, L^{n+1}]$.

3. **Numerical RG procedure.** Before detailing the RG procedure, we appeal to (4) and invoke the reputed self-similar asymptotic behavior of the solution u of (1) to write

$$L^{-n\overline{\alpha}_n} f_n\left(L^{-n\overline{\beta}_n}x\right) = u(x,L^n) \sim \frac{A}{L^{n\alpha}} f_*\left(B\frac{x}{L^{n\beta}}\right) \quad \text{as } n\to\infty. \tag{5}$$

We shall see that the RG procedure constructs the sequences $\{\alpha_n\}$, $\{\beta_n\}$, and $\{f_n\}$—thereby the sequence of renormalized IVPs (3)—so that as $n\to\infty$

- $\alpha_n \to \alpha$, $\beta_n \to \beta$;
- $A_n f_n(B_n x) = L^{n\alpha_n} u(L^{n\beta_n}x, L^n) \to A f_*(Bx)$; the scaling factors A_n and B_n will be defined shortly (see step 3 below);
- $N_n(x,t,u,p,q,\dots) \to N_*(x,t,u,p,q,\dots)$ in some sense: N_* might be given by the pointwise limit of N_n, as in the examples below; more generally, the construction of N_* might also involve some averaging, or homogenization, of N_n, as in [6].

In fact, more can be said. The limiting operator N_* is invariant under the scaling: $N_*(x,t,u,p,q,\dots) = L^{1+\alpha} N_*\left(L^\beta x, Lt, L^{-\alpha}u, L^{-(\alpha+\beta)}p, L^{-(\alpha+2\beta)}q,\dots\right)$. In other words, if $u_*(x,t)$ solves the PDE (6), then so does $L^\alpha u_*(L^\beta x, Lt)$. Furthermore, f_* is a fixed point of the RG transformation $f_* \mapsto R_{L,N_*} f_*$, where $(R_{L,N_*} f_*)(x) \equiv L^\alpha u_*(L^\beta x, L)$ is defined in terms of the solution of the IVP

$$\begin{cases} \partial_t u_* = N_*(x,t,u_*,\partial_x u_*,\partial_x^2 u_*,\dots), \quad x\in\mathbb{R},\ t>1, \\ u_*(x,1) = f_*(x), \quad x\in\mathbb{R}. \end{cases} \tag{6}$$

That is, $f_*(x) = L^\alpha u_*(L^\beta x, L)$ and the solution u_* is self-similar.

We now describe in detail the numerical RG procedure. Start with $f_0 = f$, the initial condition of the IVP (1). For $n = 0, 1, 2, \dots$, we have the following four steps:

1. Evolve u_n from $t = 1$ to $t = L$ using (3) and compute α_{n+1} so that
$$L^{\alpha_{n+1}} = \frac{\|u_n(\cdot,1)\|_\infty}{\|u_n(\cdot,L)\|_\infty} = \frac{\|u(L^{n\overline{\beta}_n}\cdot, L^n)\|_\infty}{\|u(L^{n\overline{\beta}_n}\cdot, L^{n+1})\|_\infty}.$$
2. Compute β_{n+1} from an appropriate *scaling relation*, $\beta_{n+1} = h(\alpha_{n+1})$; this idea will be elaborated below.
3. Compute $A_n = L^{n(\alpha_n - \overline{\alpha}_n)}$ and $B_n = L^{n(\beta_n - \overline{\beta}_n)}$.
4. Define $f_{n+1}(x) = (R_{L,N_n} f_n)(x) \equiv L^{\alpha_{n+1}} u_n\left(L^{\beta_{n+1}}x, L\right)$.

The following discussion amplifies some of the ideas in the above steps. The rationale behind the manner we construct $\{\alpha_n\}$ in step 1 is the self-similar asymptotic behavior we want to compute. We measure the decay of u_n (equivalently, of u) over the time-interval $[1, L]$ (equivalently, $[L^n, L^{n+1}]$) in terms of the exponent α_{n+1}. Appealing to (5), it is then expected that $L^{\alpha_{n+1}} \to L^{\alpha}$ as $n \to \infty$; that is $\alpha_{n+1} \to \alpha$.

Whereas the determination of $\{\alpha_n\}$ can always be performed as in step 1 above, the determination of $\{\beta_n\}$ is problem dependent. It usually employs a relation between the exponents α_n and β_n which is determined so that certain (a priori chosen) parts of the differential operator under study remain invariant under the scaling of step 4. We illustrate this point in an example:

$$\partial_t u = \nu\, \partial_x^2 \left(u^{1+m}\right) + \kappa\, u^p \left(\partial_x u\right)^q . \tag{7}$$

Here $\nu > 0$, κ, m, p, and q are given constants. Let us consider one iteration of the RG procedure using the above equation. Given exponents α and β, the scaling in step 4 to define $u_L(x,t) \equiv L^{\alpha} u(L^{\beta}x, Lt)$—and the IVP it satisfies to be used in the next iteration—renormalizes the coefficients of equation (7):

$$\nu \mapsto \nu_L = \nu\, L^{1-m\alpha-2\beta}, \quad \kappa \mapsto \kappa_L = \kappa\, L^{1+(1-p-q)\alpha-q\beta}. \tag{8}$$

The choice of how to determine β is dictated by what one wants to investigate. For instance, if the focus is the flow associated with the equation $\partial_t u = \nu \partial_x^2 \left(u^{1+m}\right)$, β is chosen according to the scaling relation $1 - m\alpha - 2\beta = 0$. In this way, $\nu_L = \nu$ and $\partial_t u = \nu \partial_x^2 \left(u^{1+m}\right)$ remains unchanged under the scaling.

Once this choice is exercised, one of three possible cases occurs for κ_L, depending on the relative importance of the term $u^p \left(\partial_x u\right)^q$ in the *asymptotic* flow of (7). If this term is dominated by $\partial_x^2 \left(u^{1+m}\right)$—the *irrelevant* case—, $|\kappa_L| < |\kappa|$ after sufficiently many iterations (i.e., in the asymptotic regime), so that κ_L iterates to zero. In other words, the asymptotic flow of (7) is governed by the simpler equation $\partial_t u = \nu \partial_x^2 \left(u^{1+m}\right)$. If $u^p \left(\partial_x u\right)^q$ balances $\partial_x^2 \left(u^{1+m}\right)$—the *marginal* case—, $\kappa_L = \kappa$ (i.e., $1 + (1-p-q)\alpha - q\beta = 0$) asymptotically and equation (7) does not reduce to a simpler one. Finally, if $u^p \left(\partial_x u\right)^q$ dominates over $\partial_x^2 \left(u^{1+m}\right)$—the *relevant* case—$|\kappa_L| > |\kappa|$ in the asymptotic regime. In this circumstance, β should be chosen to satisfy $1 + (1-p-q)\alpha - q\beta = 0$, which would then force $\kappa_L = \kappa$ and ν_L to iterate to zero allowing the asymptotic flow of the equation $\partial_t u = \kappa u^p \left(\partial_x u\right)^q$ to be investigated.

We emphasize that the classification of $u^p \left(\partial_x u\right)^q$ as irrelevant, marginal, or relevant is relative to the operator $\partial_x^2 \left(u^{1+m}\right)$; moreover, this classification depends on the class of initial data being considered. The latter observation will be illustrated below with numerical experiments.

In the numerical implementation of the RG procedure, the spatial scaling in step 4 can be realized in two different ways: by scaling the mesh size Δx without changing the discrete sites $j = 0, \pm 1, \ldots$, so that after one iteration the new mesh size is $(\Delta x)_1 = L^{-\beta_1} \Delta x$ and the new mesh points are located at $x = jL^{-\beta_1}\Delta x$ (this is the approach suggested in [13]) or by scaling the discrete sites while keeping the mesh size fixed, so that after one iteration the new discrete sites $L^{-\beta_1} j$ are located at $x = L^{-\beta_1} j \Delta x$. In the latter, the values of the solution u at the fixed mesh points $x = j\Delta x$ have to be interpolated from the data given at the (new) discrete sites in each iteration. This interpolation-resampling strategy was previously proposed in [27] as a means to capture the consequences of space-time translational symmetry on a discrete lattice.

The former approach is more accurate, but computationally more demanding since the reduction of Δx requires a corresponding reduction of the time-step Δt to preserve stability, rendering the evolution step 1 in the procedure progressively more expensive. So far, our experience indicates that this approach is rarely needed (we refer to [6] for an example). In particular, it is not used in this paper.

4. **Numerical experiments.** In this section we apply the numerical RG procedure described above to two sample problems. First, we explore the self-similar asymptotic decay of solutions of Burgers equation to exhibit, on one hand, the precision of the RG method to determine scaling exponents and profile functions—including scaling factors associated with inherent conservation laws—and, on the other hand, its unique capability to reveal the dominant effects in the asymptotic regime. Next, we study the anomalous asymptotic decay of solutions of a reaction-diffusion system that arises in modeling isothermal chemical reactions to illustrate the ability of the RG method to detect and compute accurately logarithmic corrections to the asymptotics.

4.1. **Burgers equation.** Burgers equation, which we write as

$$\partial_t u = \nu\, \partial_x^2 u + \kappa\, u \partial_x u, \quad x \in \mathbb{R},\, t > 0; \qquad u(x,1) = f(x), \quad x \in \mathbb{R}, \tag{9}$$

is arguably the simplest equation combining both nonlinear propagation effects and diffusive effects. We have taken $\nu = 0.01$ and $\kappa = -2$. First, we set $f(x) = \chi_{[-\ell,\ell]}(x)$, the characteristic function of the interval $[-\ell, \ell]$. It is well known [28] that solutions of (9) corresponding to nonnegative initial data with compact support evolve to a self-similar profile,

$$u(x,t) \sim \frac{1}{\sqrt{t}} \phi\left(\frac{x}{\sqrt{t}}; \frac{M}{\nu}\right), \quad \text{as } t \to \infty,$$

which is given by the 'source-type' solution of (9) when $u(x,1) = M\,\delta(x)$. A significant point to note is that the area under the profile remains constant in time, since the mass $M = \int u(x,t)\,dx$ is an invariant of the evolution.

To perform step 1 of the RG procedure, we solve (9)—and its renormalized versions— numerically using a simple explicit finite difference scheme that combines Euler's method for the time discretization with the standard three-point formula for the discretization of the second-order spatial derivative and centered differences for the first-order one. Given the stability constraints, the resulting scheme is second-order accurate.

Figure 1 depicts the fast convergence of the computed exponent α_n to the theoretical value $\alpha = 1/2$ as the numerical RG transformation is iterated. Also shown is the convergence of the computed scaling factor A_n to the theoretical value A. The value of A is determined by the mass of the initial condition, which is conserved in the evolution, and the normalization of the computed profiles f_n imposed by the numerical RG procedure (cf. step 4 above). We remark that we fix $\beta_n = 1/2$; this choice keeps the diffusion term $\nu\partial_x^2 u$ unchanged under the iteration of the RG transformation.

Figure 2 displays other aspects of the asymptotics computed by the RG procedure. In the right frame we plot $\|f_n - f_{n-1}\|_\infty / \|f_n\|_\infty$ as a function of the number of RG iterations n. The fast convergence to zero of the relative difference between successive profiles constitutes undisputable evidence of the convergence of f_n. In the left frames we plot $\kappa_n = \kappa L^{n(1/2-\overline{\alpha}_n)}$ vs. n (cf. (8)) and the superposition of the last computed profile f_n with the theoretical profile. The convergence of κ_n

to a nonzero value indicates that, for the class of initial data considered ($f(x) \geq 0$ with compact support), the nonlinear term $u\partial_x u$ is marginal relative to the diffusive term $\partial_x^2 u$. Thus the long-term effects of nonlinearity and diffusion on the decay of solutions are commensurate. This is not always the case, as our next example will show.

We now take as the initial data $f(x) = -\chi_{[-\ell,0]}(x) + \chi_{[0,\ell]}(x)$, an odd function. The results obtained with the numerical RG procedure are shown in Figures 3 and 4. In Figure 3 we plot α_n and κ_n as functions of the number of RG iterations n. In marked contrast with the previous example, κ_n now converges to zero. This is a consequence of diffusion becoming the dominant effect in the final decay of solutions. In other words, when the initial data is an odd function, the nonlinear term is irrelevant relative to diffusion. As a result, the asymptotic decay in this case is given by a dipole, a self-similar solution of the *diffusion equation* [28]:

$$u(x,t) \sim \frac{A}{t}\frac{x}{\sqrt{t}} e^{-x^2/4\nu t}, \quad \text{as } t \to \infty.$$

This is exactly what we observe in our numerical results; namely, α_n converges to 1 (Figure 3) and $f_n(x) \to \sqrt{2}\,\nu\, x\, e^{-x^2/4\nu}$ (Figure 4). (The factor $\sqrt{2}\,\nu$ results from the scaling in step 4 of the RG procedure, which forces $\|f_n\|_\infty = \|f\|_\infty = 1$.) An interesting fact to notice is the existence of a wide plateau, at a value about 1/2, in the plot for α_n. This means that the solution u decays for a long period at an almost constant rate proportional to $1/\sqrt{t}$. A typical profile f_n during this period is shown in Figure 4. It resembles an N-wave, a self-similar solution of the *inviscid* Burgers equation (see, e.g., [28] for a discussion of N-waves). So, the numerical results suggest the following picture of the decay: In an early, albeit long, stage, the decay is well described by a self-similar solution of the inviscid equation (i.e., the nonlinear term is the dominant term); eventually the diffusion term becomes dominant and the decay crosses over to that one inflicted by the diffusion equation. This picture is confirmed by an asymptotic analysis; see [28].

4.2. **Reaction-diffusion system.** We now turn our attention to the following reaction-diffusion system with cubic nonlinearity:

$$\begin{aligned} \partial_t v &= \partial_x^2 v - \lambda\, v^q u^p, \\ \partial_t u &= d\,\partial_x^2 u + \lambda\, v^q u^p, \end{aligned} \qquad q+p=3, \quad 1 \leq q,p \leq 2, \tag{10}$$

with initial conditions $v(x,1) \geq 0$ and $u(x,1) \geq 0$ having compact support. Here d and λ are positive constants. This system arises as a model for cubic autocatalytic chemical reactions of the type $q\,R + p\,C \longrightarrow 3\,C$, see [5] and references therein; v is the concentration of reactant R, u is that of autocatalyst C.

The large-time decay of solutions of (10) is studied in [10], when $q = 1$ and $p = 2$, and in [23], when $1 < q, p < 2$. We have been able to reproduce in detail their theoretical results using the numerical RG procedure described above. In the following, we present our numerical results when $q = p = 1.5$, $d = 0.75$, and $\lambda = 1$. Our intent is to illustrate the remarkable ability of the RG procedure to uncover and compute accurately logarithmic corrections to the decay. For reference, we state (somewhat loosely) the main result of Li-Qi [23]:

$$\begin{aligned} &\sqrt{t}\,(\log t)^{\frac{1}{q-1}}\; v(\sqrt{t}\,x,t) \sim B/\sqrt{4\pi}\, e^{-x^2/4}, \\ &\sqrt{t}\,u(\sqrt{t}\,x,t) \sim A/\sqrt{4\pi d}\, e^{-x^2/4d}, \end{aligned} \quad \text{as } t \to \infty, \tag{11}$$

where $B = B(A, d, q, p)$ is determined explicitly and $A = \int (v(x,1) + u(x,1))\, dx$ is the total mass, which is conserved in time.

Figures 5 and 6 depict some of the aspects of the asymptotics (11) as computed by the numerical RG procedure. We note in passing that the RG procedure computes a set of scaling exponents, factors and profiles for each of the two components of the system, v and u; we use subscripts to distinguish the sets. Also, we remark that we fix the exponents $\beta_{v,n} = \beta_{u,n} = 1/2$ to keep the diffusion terms invariant. For the discretization of system (10), we employ the same numerical scheme we used for Burgers equation.

In regard to Figure 5, we make two observations. First, we note the disparate rates with which the computed decay exponents, $\alpha_{v,n}$ and $\alpha_{u,n}$, converge to 1/2: The former converges much slower. Second, we point out the peculiar convergence of the scaling factor $A_{v,n}$ to zero. Since

$$A_{v,n}\, f_{v,n}(x) = L^{n\alpha_{v,n}}\, v(L^{n/2}\, x, L^n)$$

(see the second bullet in Section 3), these observations can be interpreted as the signature of a departure from power-law decay. To test this conjecture, we analyze the convergence of $A_{v,n}$ in a log-log plot, shown in Figure 5. It is evident that $A_{v,n} \sim A_* \,(\log L^n)^{-2}$, as $n \to \infty$. Therefore, the computed results furnish the following portrait of the asymptotic decay:

$$\begin{aligned} v(x, L^n) &\sim \frac{A_*}{L^{n/2}\,(\log L^n)^{\alpha}}\, \phi_v\left(\frac{x}{L^{n/2}}\right), \quad \text{with } \alpha = 2, \\ u(x, L^n) &\sim \frac{A_u}{L^{n/2}}\, \phi_u\left(\frac{x}{L^{n/2}}\right), \end{aligned} \tag{12}$$

as $n \to \infty$. We mention that the computed limiting profiles, ϕ_v and ϕ_u, are indeed the Gaussians displayed in (11). Also, the limiting scaling factor A_u matches very closely the theoretical value A in (11), which is given by the total mass.

Next, we present a modified version of the RG procedure which is suitable for the computation of asymptotics in the form (12). In this version, the exponent α and scaling factor A_* are calculated explicitly. The specifics follow.

To reflect the presence of the logarithmic correction to the decay and to allow the explicit computation of α, step 1 of the modified version reads:

1. Evolve v_{n-1} from $t = 1$ to $t = L$ and compute α_n so that

$$L^{1/2}\left(\frac{n}{n-1}\right)^{\alpha_n} = \frac{\|v_{n-1}(\cdot, 1)\|_\infty}{\|v_{n-1}(\cdot, L)\|_\infty} \quad (n \geq 2). \tag{13}$$

This modification, in turn, entails the following changes in steps 3 and 4 of the RG procedure (cf. Section 3):

3. $A_n = L^{\frac{1}{2}-\alpha_1} \prod_{k=2}^{n} [n/(n-1)]^{\alpha_n - \alpha_k}$. (14)
4. $v_n(x, 1) = L^{1/2}\, [n/(n-1)]^{\alpha_n}\, v_{n-1}\left(L^{1/2}\, x, L\right)$.

(α_1 and v_1 are computed with the 'standard' RG approach described in Section 3.)

Figure 7 shows the convergence of α_n to 2 and of A_n to the theoretical value B in (11), when the modified RG procedure is applied to system (10).

We emphasize that the crucial feature which enables the RG procedure to uncover corrections to a power-law decay is the information encapsulated in the convergence of the scaling factor A_n, as computed in Section 3. In this regard the numerical RG procedure is similar to the 'dynamic rescaling' method introduced in [22].

5. **Concluding remarks.** We have presented a systematic numerical procedure, based on the RG approach, for the detailed and efficient computation of asymptotically self-similar dynamics. The effectiveness of the method was illustrated in a couple of nonlinear PDEs combining diffusive, reactive and nonlinear propagation effects. We refer to [21] for additional examples of the success of the method, including cases of multidimensional problems.

Proper modifications of the RG procedure that we described have also been used for the computation of traveling waves [13], [7]. We are currently investigating the applicability of an adapted version of the method to blow-up problems; we expect to report our results in the near future.

Acknowledgements. F.F. owes a great debt of gratitude to Nigel Goldenfeld and Yoshitsugu Oono for their hospitality and willingness to teach him the renormalization group method.

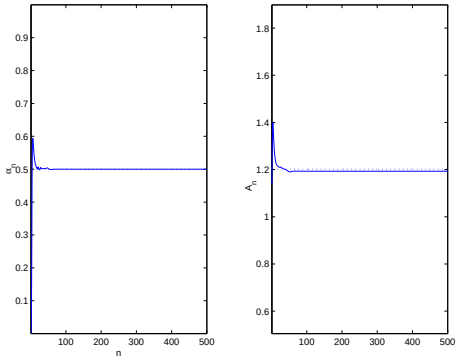

FIGURE 1. Convergence of α_n (left frame) and A_n (right frame) to their respective theoretical values (dotted lines) as the RG map is iterated, in the case of Burgers equation with $f(x) = \chi_{[-\ell,\ell]}(x)$.

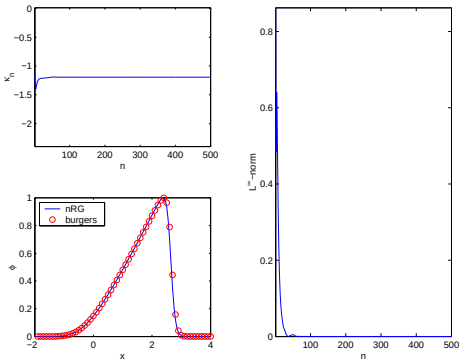

FIGURE 2. Left frames: κ_n vs. n (top) and the last computed profile f_n with the theoretical profile (circles) superposed (bottom). Right frame: $\|f_n - f_{n-1}\|_\infty / \|f_n\|_\infty$ vs. n. These results refer to Burgers equation with $f(x) = \chi_{[-\ell,\ell]}(x)$.

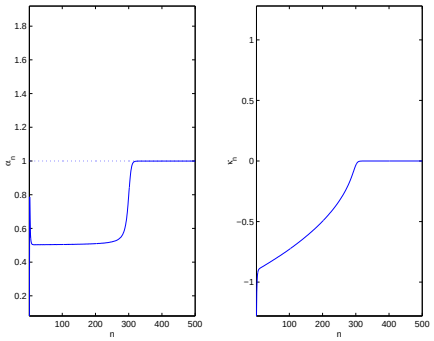

FIGURE 3. α_n (left) and κ_n (right) as functions of the number of RG iterations n for Burgers equation with $f(x) = -\chi_{[-\ell,0]}(x) + \chi_{[0,\ell]}(x)$.

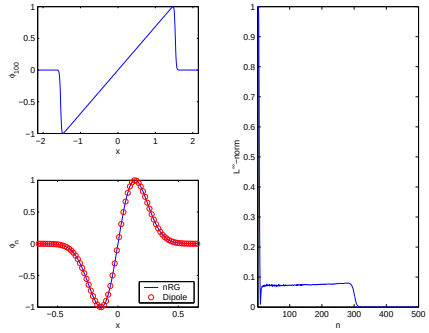

FIGURE 4. Left frames: N-wave-like profile after 100 RG iterations (top); last computed profile f_n with the dipole (circles) superposed (bottom). Right frame: $\|f_n - f_{n-1}\|_\infty / \|f_n\|_\infty$ vs. n. These results pertain to Burgers equation with $f(x) = -\chi_{[-\ell,0]}(x) + \chi_{[0,\ell]}(x)$.

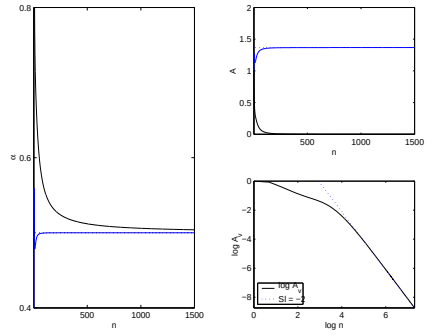

FIGURE 5. Left frame: Exponents $\alpha_{v,n}$ (black) and $\alpha_{u,n}$ (blue) vs. the number of RG iterations n. Right frames: $A_{v,n}$ (black) and $A_{u,n}$ (blue) vs. n (top); $A_{v,n}$ vs. n in log-log scale (bottom).

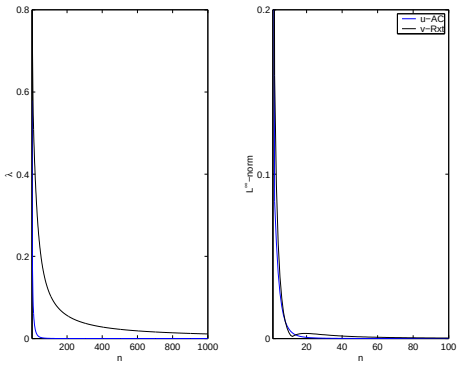

FIGURE 6. Convergence of $\lambda_{v,n}$ and $\lambda_{v,n}$ (left); and of relative differences in successive profiles $f_{v,n}$ and $f_{u,n}$ (right) as the RG map is iterated.

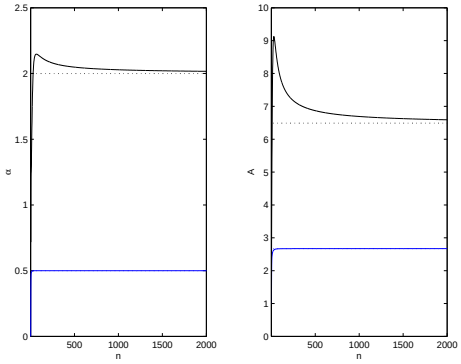

FIGURE 7. Left frame: Exponents α_n (cf. (13)) (black) and $\alpha_{u,n}$ (blue) computed by the modified RG procedure. Right frame: Prefactors A_n (cf. (14)) (black) and $A_{u,n}$ (blue) computed by the modified RG procedure. The dotted lines are theoretical values.

REFERENCES

[1] S. B. Angenent, D. G. Aronson, S. I. Betelu, and J. S. Lowengrub, *Focusing of an elongated hole in porous medium flow*, Phys. D, **151** (2001), 228–252.
[2] G. I. Barenblatt, "Scaling", Cambridge University Press, Cambridge, 2002.
[3] M. Berger and R. Kohn, *A rescaling algorithm for the numerical calculation of blowing-up solutions*, Comm. Pure Appl. Math., **1** (1988), no. 6, 841–863.
[4] S. I. Betelu, D. G. Aronson, and S. B. Angenent, *Renormalization study of two-dimensional convergent solutions of the porous medium equation*, Phys. D, **138** (2000), 344–359.
[5] J. Billingham, and D. J. Needham, *The development of traveling waves in quadratic and cubic autocatalysis with unequal diffusion rates. I. Permanent form traveling waves*, Phil. Trans. R. Soc. Lond. A, **334** (1991), 1–24.
[6] G. A. Braga, F. Furtado, J. M. Moreira, and L. T. Rolla, *Renormalization group analysis of nonlinear diffusion equations with periodic coefficients*, SIAM Multiscale Model. Simul., **1** (2003), no. 4, 630–644.
[7] G. A. Braga, F. Furtado, V. Isaia, and L. T. Rolla, *in preparation* (2004).

[8] J. Bricmont, A. Kupiainen, *Renormalizing partial differential equations*, Constructive Physics, Berlin: Springer, Lecture Notes in Physics, **446** (1995), 83-115.
[9] J. Bricmont, A. Kupiainen and G. Lin, *Renormalization group and asymptotics of solutions of nonlinear parabolic equations*, Comm. Pure Appl. Math., **47** (1994), 893-922.
[10] J. Bricmont, A. Kupiainen, and J. Xin, *Global large time self-similarity of a thermal-diffusive combustion system with critical nonlinearity*, J. Diff. Eqns., **130** (1996), 9–35.
[11] G. Caginalp, *Renormalization and scaling methods for nonlinear parabolic systems*, Nonlinearity, **10** (1997), 1217–1229.
[12] G. Caginalp, *A renormalization group approach to blow-up and extinction exponents*, Nonlinear Analysis, **47** (2001), 2187–2202.
[13] L. Chen, N. Goldenfeld, *Numerical renormalization group calculations for similarity solutions and traveling waves*, Phys. Rev., **51** (1995), 5577-5581.
[14] L. Chen, N. Goldenfeld, and Y. Oono, *Renormalization-group theory for the modified porous-medium equation*, Phys. Rev. A, **44** (1991), 6544–6550.
[15] A. J. Chorin, O. H. Hald, and R. Kupferman, *Prediction from partial data, renormalization, and averaging*, preprint, available at http://math.berkeley.edu/∼chorin.
[16] G. Fibich and X. P. Wang, *Stability of solitary wave for nonlinear Schrödinger equations with inhomogeneous nonlinearities*, Phys. D, **175** (2003), 96–108.
[17] M. Gell-Mann and F. E. Low, *Quantum electrodynamics at small distances*, Phys. Rev., **95** (1954), 1300-1312.
[18] N. Goldenfeld, Lectures on Phase Transitions and the Renormalization Group, Reading: Addison-Wesley, 1992.
[19] N. Goldenfeld, O. Martin, Y. Oono, and F. Liu, *Anomalous dimensions and the renormalization group in a nonlinear diffusion process*, Phys. Rev. Lett., **65** (1990), 1361–1364.
[20] N. Goldenfeld, O. Martin, and Y. Oono, *Asymptotics of partial differential equations and the renormalization group*, Proc. NATO Advanced Research Workshop on Asymptotics Beyond All Orders, S. Tanveer, ed. (Plenum, New York, 1992).
[21] V. Isaia, Intermediate Asymptotic Behavior of Nonlinear Parabolic PDEs via a Renormalization Group Approach: a Numerical Study, Ph.D. thesis, Department of Mathematics, University of Wyoming, 2002.
[22] B. LeMesurier, G. Papanicolaou, C. Sulem, and P.-L. Sulem, *The focusing singularity of the cubic Schrödinger equation*, Phys. Rev. A, **34** (1986), 1200–1210.
[23] Y. Li and Y. W. Qi, *The global dynamics of isothermal chemical systems with critical nonlinearity*, Nonlinearity, **16** (2003), 1057–1074.
[24] S. K. Ma, "Modern Theory of Critical Phenomena", Reading: Benjamin/Cummings Publishing Company, 1976.
[25] H. Merdan and G. Caginalp, *Decay of solutions to nonlinear parabolic equations: renormalization and rigorous results*, DCDS-B, **3** (2003), 565-588.
[26] W. Ren and X. P. Wang, *An iterative grid redistribution method for singular problems in multiple dimensions*, J. Comp. Phys., **159** (2000), 246–273.
[27] L. San Martin and Y. Oono, *Physics-motivated numerical solvers for partial differential equations*, Phys. Rev. E, **57** (1998), 4795–4810.
[28] G. B. Whitham, "Linear and Nonlinear Waves", Wiley-Intersciences, New York, 1973.
[29] K. Wilson, *Renormalization group and critical phenomena I - II*, Phys. Rev. B, **4** (1971), 3174–83, 3184–3205.

Received September, 2004; revised April, 2005.

E-mail address: gbraga@mat.ufmg.br
E-mail address: furtado@uwyo.edu
E-mail address: isaiavm@alfredstate.edu